Low-energy electron scattering by CF_4, CCl_4, $SiCl_4$, $SiBr_4$, and SiI_4

Márcio T. do N. Varella, Alexandra P. P. Natalense,* Márcio H. F. Bettega, and Marco A. P. Lima
Instituto de Física ''Gleb Wataghin,'' Universidade Estadual de Campinas, Unicamp, 13083-970 Campinas, São Paulo, Brazil and Departamento de Física, Universidade Federal do Paraná, Caixa Postal 19081, 81531-990 Curitiba, Paraná, Brazil
(Received 1 September 1998; revised manuscript received 12 July 1999)

In this paper, we show elastic and rotationally inelastic cross-section calculations of low-energy electron scattering by CF_4, CCl_4, $SiCl_4$, $SiBr_4$, and SiI_4. The fixed-nuclei static-exchange scattering amplitudes were obtained with the Schwinger multichannel method with soft norm-conserving pseudopotentials. We show elastic integral and differential cross sections and discuss the role of the basis set on the nature of some structures seen in a previous publication [A. P. P. Natalense *et al.*, Phys. Rev. A **52**, R1 (1995)]. We have attributed these structures to linear dependency in the basis set caused by the symmetric combination $(x^2+y^2+z^2)\exp(-\alpha r^2)$. The rotational cross sections were calculated with the help of the adiabatic-nuclei-rotation approximation. Our results are in good agreement with available experimental data. The sums of $0 \rightarrow 0,3,4,6$ rotational cross sections in general show good agreement with the elastic (rotationally unresolved) ones. The rotationally summed integral cross section agrees within 0.3% with the elastic integral cross section for CF_4 at 7.5 eV, and within 26% for SiI_4 at 30 eV. It was found that rotationally inelastic cross sections are considerably large for such molecules, because the heavy peripheral atoms play a significant role as scattering centers. [S1050-2947(99)00611-3]

PACS number(s): 34.80.Bm, 34.80.Gs

I. INTRODUCTION

Recently, studies on collisions of low-energy electrons with molecules have experienced great improvement, especially for molecules such as CH_4, SiH_4, CCl_2F_2, CF_4, CCl_4, etc. [1]. The resulting cross sections play an important role in the modeling of cold plasmas. In these plasmas ''hot'' electrons collide with ''cold'' molecules generating ions, atoms, and radicals which are responsible for industrially interesting processes (etching, polimerization, nitriding, etc.). However, calculation of scattering cross sections for large molecules by *ab initio* methods quickly reaches computational limitations.

The *ab initio* methods in current use that are able to deal with molecules with arbitrary geometries are the Schwinger multichannel (SMC) method [2], the complex Kohn variational method [3], and the polyatomic version of the *R*-matrix method [4]. In this paper, we discuss in detail the results obtained using the Schwinger multichannel method in conjuction with norm-conserving pseudopotentials (SMCPP) [5]. This combined method allows studies on molecules with hundreds of electrons. The basic idea involved in this procedure is to replace the core electrons and the nucleus of each atom in the molecule by the corresponding soft norm-conserving pseudopotential and to describe the valence electrons in a many-body framework (Hartree-Fock approximation in the present implementation). The resulting atomic wave functions are nodeless and smooth and can be expanded in smaller basis sets. Furthermore, these norm-conserving pseudopotentials were designed to work in different environments (atoms, molecules, solids) [6] and we have shown that the SMCPP can provide very good results in many different situations as bound-state calculations [5] and scattering calculations in different approximations (elastic [5,7,8], electronic excitations by electron impact [9,10], and rotational excitation cross sections [11,12]).

This is a full length paper, which includes the results of a previous Rapid Communication [7] together with new results for differential, partial, and rotational excitation cross sections for CF_4, CCl_4, $SiCl_4$, $SiBr_4$, and SiI_4. Here we are dealing with the static-exchange approximation, which we regard as an initial step towards more elaborate calculations including electronic excitations and polarization effects. These fixed-nuclei elastic scattering amplitudes, however, can be readily used to obtain rotational excitation cross sections through the adiabatic-nuclei-rotation (ANR) approximation. This approach, combining scattering amplitudes obtained with the help of pseudopotentials and the ANR approximation, has been successfully applied to moderately large molecules (CH_4, SiH_4, GeH_4, PbH_4 [11] and NH_3, PH_3, AsH_3, SbH_3 [12]) and we are now extending its application to larger systems.

As pointed out by Jung *et al.* [13], pure rotational energy transfer from electrons to molecular gases is often quite effective. Even though the energy transfer per collision is quite small for polyatomic molecules, the cross sections are very large, 10^{-16} cm^2 or even more. In spite of their importance for these cold plasmas, we were not able to find rotationally resolved cross sections reported for the molecules studied in this paper. Theoretical works are mainly restricted by the computational limitations referred to above, whereas experimentalists run up against insufficient resolution of experimental devices. Müller *et al.* [14] have reported experimental rotationally resolved cross sections for methane. Those measurements took advantage of a broadening, caused by pure rotational excitations, of energy-loss peaks. However, since

*Present address: Department of Chemistry, Texas A& M University, College Station, TX 77843-3255.

the separation between neighboring rotational levels of CH_4 is typically of 10^{-4} eV, whereas it is about $10^{-6}-10^{-5}$ eV for the heavier molecules treated here, we are not sure about the possibility of extending their approach to these larger systems. We believe that such a lack of relevant rotationally resolved cross sections in the literature makes our effort worthwhile. We report state-to-state cross sections, departing from the rotational ground state of the targets ($J=0\rightarrow J'=0,3,4,6$). Such state-to-state cross sections are the fundamental information concerning pure rotational energy transfer in gaseous discharges. Any rotational cross section ($J\rightarrow J'$) can be extracted from $J=0\rightarrow J'$ state-to-state ones [15]. As a result, if one knows the population of rotational states of the molecular gas at a given temperature, any physical quantity concerning rotational excitations—such as momentum transfer and energy-loss cross sections—can be obtained by averaging over the population distribution.

The rotational resolution of the cross sections may still be regarded as a more detailed test for the pseudopotential approach, and also as a good opportunity to observe the influence of the external atoms in the scattering process. We are dealing with two types of central atoms (C and Si) and four types of peripheral atoms (F, Cl, Br, and I).

This paper is outlined as follows. Our method is described in Sec. II. Next, in Sec. III, we show our total, differential, and partial cross sections, compared to the theoretical and experimental data available in the literature, and present some discussions about our results. Rotational results are also included in this section. The conclusions are written in Sec. IV.

II. METHOD

A. Elastic cross sections

To calculate elastic cross sections for CF_4, CCl_4, $SiCl_4$, $SiBr_4$, and SiI_4, we used the Schwinger multichannel method (SMC) [2,16] with the pseudopotentials [5] of Ref. [6]. The SMC method has been previously described and we only review here some key features for completeness. In this method, the resulting expression for the scattering amplitude is

$$[f_{\vec{k}_i,\vec{k}_f}]=-\frac{1}{2\pi}\sum_{m,n}\langle S_{\vec{k}_f}|V|\chi_m\rangle(d^{-1})_{mn}\langle\chi_n|V|S_{\vec{k}_i}\rangle, \quad (1)$$

where

$$d_{mn}=\langle\chi_m|A^{(+)}|\chi_n\rangle \quad (2)$$

and

$$A^{(+)}=\frac{\hat{H}}{N+1}-\frac{(\hat{H}P+P\hat{H})}{2}+\frac{(VP+PV)}{2}-VG_P^{(+)}V. \quad (3)$$

In the above equations, $S_{\vec{k}_i}$ is the product of a target state and a plane wave, V is the interaction potential between the incident electron and the target, χ_m is an $(N+1)$-electron Slater determinant used in the expansion of the trial scattering wave function, $\hat{H}$ is the total energy of the collision minus the full Hamiltonian of the system, P is a projection operator onto the open-channel space defined by target eigenfunctions, and $G_P^{(+)}$ is the free-particle Green's function projected on the P space.

In the present formulation, where Cartesian Gaussian functions are used to represent atomic, molecular, and scattering orbitals, all matrix elements needed to evaluate the scattering amplitude are computed analytically, except those involving the Green's function ($\langle\chi_m|VG_P^{(+)}V|\chi_n\rangle$), which are calculated by numerical quadrature [17].

In the SMC method, the most expensive step is the generation of matrix elements of the VGV term, which needs the evaluation of primitive two-electron integrals

$$\langle\alpha\beta|V|\gamma\vec{k}\rangle=\int\int d\vec{r}_1 d\vec{r}_2\,\alpha(\vec{r}_1)\beta(\vec{r}_1)\frac{1}{r_{12}}\gamma(\vec{r}_2)e^{i\vec{k}\cdot\vec{r}_2}, \quad (4)$$

involving three Cartesian Gaussian functions α, β, and γ and a plane wave $\vec{k}$. When we describe the molecular target with the help of norm-conserving pseudopotentials, our basis-set size can be reduced since we only need to describe valence pseudo-orbitals, which are smooth and nodeless functions. This fact drastically reduces the number of two-electron integrals of Eq. (4). On the other hand, we must evaluate one-electron integrals of the type

$$\langle\alpha|V^{\mathrm{PP}}|\vec{k}\rangle=\int d\vec{r}\,\alpha(\vec{r})V^{\mathrm{PP}}e^{i\vec{k}\cdot\vec{r}}, \quad (5)$$

where V^{PP} is the nonlocal pseudopotential operator [6].

These one-electron integrals are more complex than those involving the nuclei, but they can also be calculated analytically and their number is also reduced due to the smaller basis set. The overall computational saving is very meaningful and allows us to study the electron scattering by molecules containing heavy atoms.

B. Rotational cross sections

The theoretical procedure used is carefully discussed elsewhere [11,18]. The expression for the rotational cross sections, recalling that spherical-top molecules present $(2J+1)^2$ degeneracies, is

$$\frac{d\sigma}{d\Omega}(\theta'_{\mathrm{out}},J\rightarrow J')=\frac{1}{2\pi}\frac{k_{J'}}{k_J}\frac{1}{(2J+1)^2}\times\sum_{\substack{KM\\K'M'}}\int d\phi'_{\mathrm{out}}|f^{\mathrm{lab}}(\hat{k}'_{\mathrm{out}},JKM\rightarrow J'K'M')|^2, \quad (6)$$

where K is the projection of the total molecular angular momentum J on the axis of quantization in the body-fixed frame (BF), while M is the similar projection in the laboratory-fixed frame (LF). The angles θ'_{out} and ϕ'_{out} define the scattering direction in the LF ($\hat{k}'_{\mathrm{out}}$). Directions in the BF will be denoted by unprimed symbols.

The ANR expression for the rotational scattering amplitude is given by

TABLE I. Bond lengths (R) and rotational constants (B) for XY_4.

System	R (Å)	$B(10^{-6}$ eV)
CF_4	1.32	23.7
CCl_4	1.77	12.3
$SiCl_4$	2.02	5.41
$SiBr_4$	2.15	1.85
SiI_4	2.43	1.04

$$f^{\text{lab}}(\hat{k}'_{\text{out}}, JKM \rightarrow J'K'M') = \int \Psi^*_{J'K'M'}(\Omega) f^{\text{lab}}(\hat{k}'_{\text{out}}, \Omega, k_{\text{out}}, k_{\text{in}}) \Psi_{JKM}(\Omega) d\Omega. \quad (7)$$

In the above expression, $\Psi_{JKM}(\Omega)$ are rotational eigenfunctions of the target

$$\Psi_{JKM}(\Omega) = \left(\frac{2J+1}{8\pi^2}\right)^{1/2} D^{J*}_{KM}(\Omega), \quad (8)$$

TABLE II. Cartesian Gaussian function exponents for present calculations (basis A) and for the previous pseudopotential calculations [7] (basis B).

	Basis A s	Basis B s	Basis A p	Basis B p	Basis A d	Basis B d
C	11.13198	12.55600	3.745398	3.464281	0.650000	0.750000
	2.668779	2.518151	0.875034	0.724850		
	0.833043	0.575694	0.245994	0.156792		
	0.254885	0.164591	0.066435	0.060000		
	0.075554	0.040000				
Si	6.143172	12.93018	3.468604	2.413262	0.499124	0.750000
	3.207261	4.928600	0.302834	0.295707		
	1.723970	1.249363	0.091281	0.081988		
	0.176634	0.164839	0.026183	0.040000		
	0.037088	0.040000				
F	6.193838	6.566553	10.54755	9.227683	0.677371	1.288000
	1.539907	1.325552	2.312963	1.927834		
	0.457997	0.369395	0.394868	0.394868		
	0.077101	0.050000	0.060000	0.060000		
Cl	7.481548	8.059605	3.763450	3.906221	0.677371	0.457000
	2.555493	2.631167	0.657683	0.639527		
	0.388645	0.328956	0.191444	0.178773		
	0.105172	0.050000	0.043618	0.060000		
	0.037842					
Br	7.125211	6.700730	1.888852	1.962534	0.205494	0.348000
	1.541477	1.609640	0.499794	0.481668		
	0.331410	0.300758	0.153333	0.137120		
	0.097067	0.050000	0.035077	0.060000		
	0.024267					
I	2.156794	2.500000	1.214596	1.065830	0.205494	0.241000
	0.970574	1.439850	0.321194	0.365992		
	0.433010	0.239593	0.103077	0.118764		
	0.102306	0.050000	0.020360	0.040000		
	0.054860					

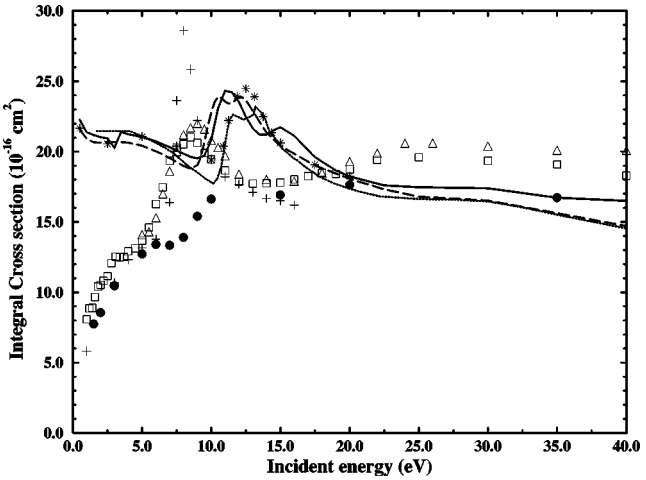

FIG. 1. Integral elastic cross section for e^--CF_4 scattering. Solid line: present pseudopotential calculation (basis A); long-dashed line: previous pseudopotential calculation (basis B) [7]; dotted line: all-electron SMC calculation [21]; stars: static-exchange CKM calculation [22]; crosses: polarized CKM calculation [22]; filled circles: experimental data [23] (elastic cross section); squares: experimental data [24] (total cross section); triangles: experimental data [25] (total cross section).

where $D^J_{KM}(\Omega)$ are Wigner rotation matrices [19].

It is to be pointed out that elastic amplitudes appearing in Eq. (7)—and calculated as in Eq. (1)—are primarily evaluated in the BF. Transformation into the LF is accomplished through expansion of the $\hat{k}_{\text{out}}$ dependence in spherical harmonics, followed by usual D-matrix rotation.

The rotational energies are calculated as

$$\frac{k_J^2}{2} = BJ(J+1) \quad (9)$$

and the rotational constants (B) are listed in Table I.

III. DISCUSSION AND RESULTS

In this work, in a first round of calculations, we have used 111 Cartesian Gaussian functions for CF_4 and 115 for the other molecules. We have performed extra calculations for CF_4 (126-function basis set), CCl_4, and SiI_4 (both with 147-function basis sets). These basis sets were chosen to be used in our pseudopotential calculations according to the method described in Ref. [20]. In Table II, we present the Gaussians' exponents for the present calculations (basis A) and also for the previous Rapid Communication [7] calculations (basis B). The diffuse functions were added to the basis sets for a better description of the scattering process.

A. Elastic results

We show, in Fig. 1, our integral elastic cross section for CF_4 (basis A). For comparison purposes, we also include the previous SMCPP results [7] (basis B), an all-electron SMC calculation [21], complex Kohn method (CKM) all-electron calculations [22], experimental results of Boesten *et al.* (elastic cross section) [23], of Sueoka *et al.* [24] (total cross section) and of Szmytkowski *et al.* (total cross section) [25]. It is clear that all SMC calculations (both pseudopotential and

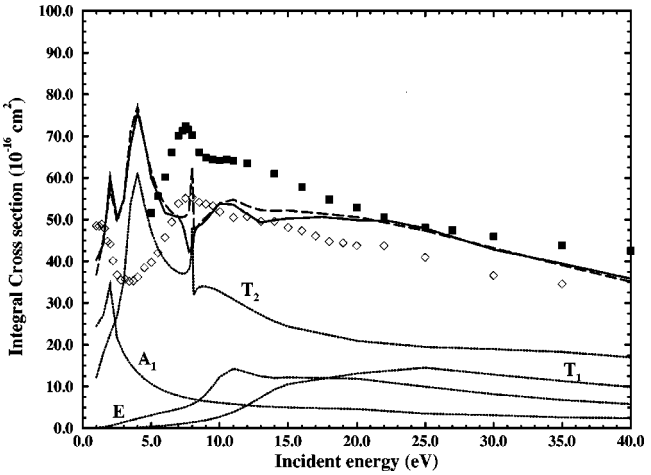

FIG. 2. Integral cross section for e^--CCl_4 scattering. Solid line: present pseudopotential calculation. Long-dashed lines: previous pseudopotential calculation [7] (integral elastic cross section). Dotted line: partial cross sections of Ref. [7]. Filled squares: experiment [25] (total cross section). Open diamonds: experiment [24] (total cross section).

all-electron) are in good agreement; the discrepancies are less than 10% at all energies. One may notice that present PP results show more spread structures between 10.0 eV and 17.0 eV and a thin structure at 3.0 eV. The latter is spurious and will be discussed further. Our results also agree very well with the CKM static-exchange (SE) calculation [22]. Though not shown here, there is a polarized potential scattering calculation of Gianturco *et al.* [26], which agrees in shape (but not in magnitude) with polarized CKM results. Our SE results agree reasonably with the experimental elastic cross section of Ref. [23] only beyond 10.0 eV.

In Figs. 2–5, we show our integral elastic cross sections (basis A) for CCl_4, $SiCl_4$, $SiBr_4$, and SiI_4, respectively. Once more, we present results of our previous calculations (basis B) [7] (including the partial cross sections, which have not been reported) and experimental data [24,25,27]. For

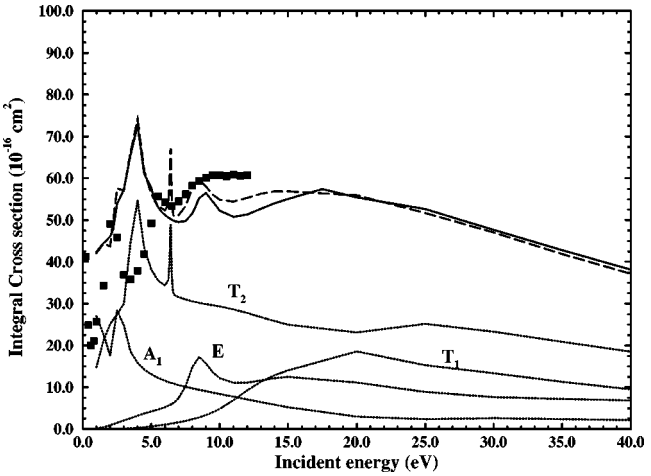

FIG. 3. Integral cross section for e^--$SiCl_4$ scattering. Solid line: present pseudopotential calculation. Dotted line: partial cross sections of Ref. [7]. Long-dashed lines: previous pseudopotential calculation [7] (partial and integral elastic cross section). Squares: experiment [27] (total cross section).

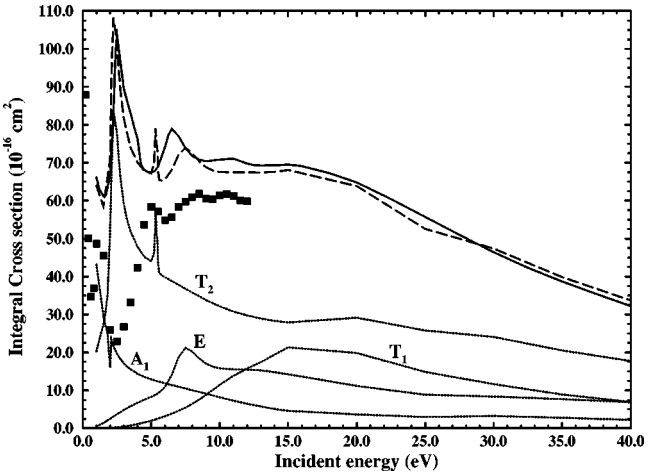

FIG. 4. Same as in Fig. 3, but for e^--$SiBr_4$ scattering.

these molecules, we could only find experimental total cross sections and this fact may be responsible for the discrepancies above 7.5 eV, since we are reporting calculated elastic cross sections. Comparing experimental (total) and calculated (elastic) cross sections, however, one always finds reasonable agreement in shape, and some structures noticed in the experiment are also found in the theoretical results, but shifted to the right. This shifting was to be expected since we are reporting static-exchange (SE) results.

The reader should note that the results of the previous work [7] present very thin structures in the integral cross sections for CCl_4, $SiCl_4$, $SiBr_4$, and SiI_4 at 8.0 eV, 6.4 eV, 5.3 eV, and 4.2 eV, respectively. Those structures may be related to numerical instabilities (spurious resonances) or to actual shape resonances. The partial cross sections undoubtedly related them to the T_2 global symmetry in all cases (see Figs. 2–5), and the eigenphase sums for this symmetry (not shown in the Rapid Communication) increased by 3π, as shown in Fig. 6, in the region of the ''resonances.'' (Remember that the T_2 symmetry is threefold degenerate, and the eigenphase sum increases by π for each degree of degeneracy.) After performing a second round of calculations using basis A (see Table II), however, it became clear that the thin structures were, in fact, spurious resonances. We believe that they are related to a linear dependency caused by the

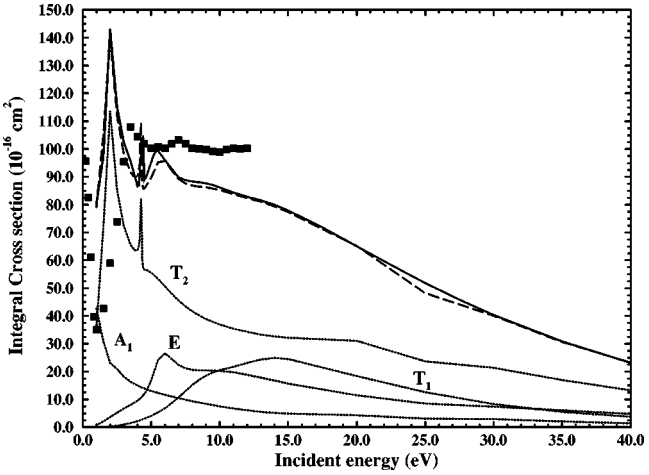

FIG. 5. Same as in Fig. 3, but for e^--SiI_4 scattering.

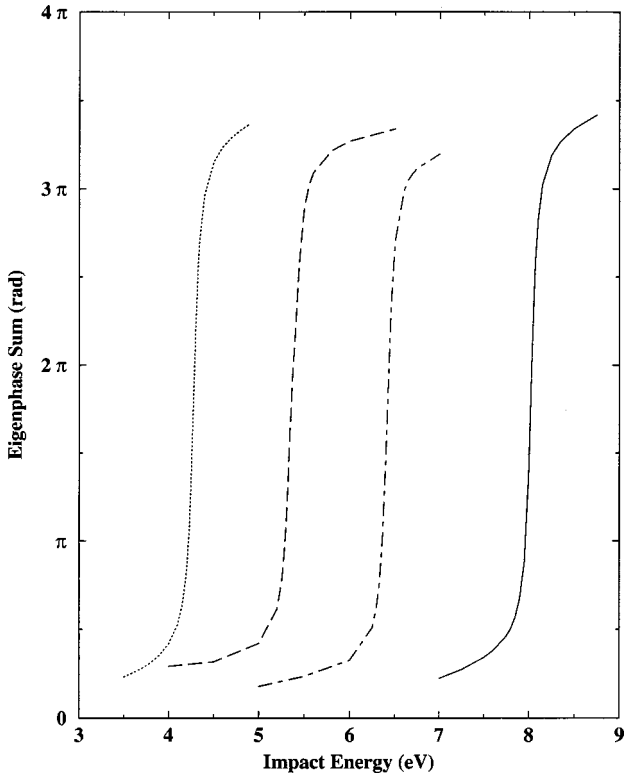

FIG. 6. Eigenphase sum for the T_2 symmetry in the region of the resonances. All results concern the basis sets Ref. [7]. Solid line: CCl_4. Dashed line: $SiCl_4$. Dot-dashed line: $SiBr_4$. Dotted line: SiI_4.

$(x^2+y^2+z^2)\exp(-\alpha r^2)$ components of the basis sets. Our belief is based on the following argument: for SiI_4, we found the spurious thin structure at 4.2 eV with both basis sets (A and B). Since our 111-function and 115-function basis sets are minimal for such a large system, it was not easy to obtain converged cross sections, and some exponents of the basis sets could not be chosen at will. In fact, for SiI_4, it was impossible to obtain good cross sections without an exponent of the *d* Gaussian function of the I atom around 0.2. For example, if we perform the calculations with a basis set identical to basis A, but changing the *d* Gaussian exponent of the I atom from 0.205 494 to 0.614 618, we obtain a cross section that is poorer than the one provided by basis A. This poorer cross section, however, does not present the thin structure. In order to verify this hypothesis, we performed once more the calculations using basis A, but this time without including the $(x^2+y^2+z^2)\exp(-\alpha r^2)$ components of the basis sets as scattering orbitals. This implies a 107-function scattering basis set, which is too small and did not show good convergence of the numerical integrals. Fortunately, very recently we improved our computational facilities and it was possible to perform calculations with a larger 159-Gaussian basis set for SiI_4, in which we have used basis A for the Si atom and the basis shown in Table III for the I atom. Since we again excluded the problematic combination, we have actually used a 147-function scattering basis set, obtaining an elastic cross section that agrees very well with the previous results (basis A and B), but without the thin structure at 4.2 eV. This entire procedure is summarized in Fig. 7, where we find the following results: (i) obtained with basis A (present); (ii) obtained with basis B [7]; (iii) obtained with basis C (which is the same as basis A with the above-referred change of the *d* Gaussian exponent); (iv) with basis D [which is the same as basis A without including the $(x^2+y^2+z^2)\exp(-\alpha r^2)$ components of the basis sets as scattering orbitals]; and (v) obtained with basis E (which is the 147-function scattering basis set).

TABLE III. Gaussian exponents for the larger basis of F, Cl, and I atoms. See text for explanation.

	s	*p*	*d*
F	12.54558	9.852550	0.677371
	6.272790	2.330403	
	1.576479	0.462593	
	0.499283	0.154197	
	0.150680	0.051399	
	0.077101		
Cl	10.49065	6.037205	1.611766
	6.836599	2.012401	0.328314
	2.420592	0.686842	
	0.513579	0.218056	
	0.188863	0.071193	
	0.062954		
	0.015738		
I	7.416182	2.328646	0.275211
	2.192460	1.450975	0.099270
	1.067534	0.368373	
	0.610606	0.144575	
	0.197322	0.055983	
	0.068478		
	0.021562		

For CCl_4 (Fig. 2), the present calculation also shows a thin structure at 8.0 eV, but, in comparison to the thin structure of the previous calculation [7], it is inverted. Such structure is also spurious. We have performed another calculation

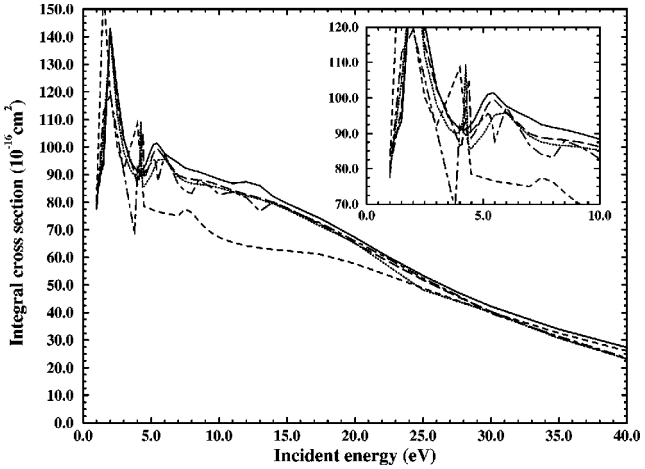

FIG. 7. Integral cross section for e^--SiI_4 scattering. Solid line: basis E (147-function calculation). Long-dashed line: basis A (115-function calculation). Dotted line: basis B (111-function calculation [7]). Dashed line: basis C (same as basis A with a change in the *d* Gaussian exponent). Dot-dashed line: basis D (109-function calculation, excluding the symmetric *d* Gaussian combination).

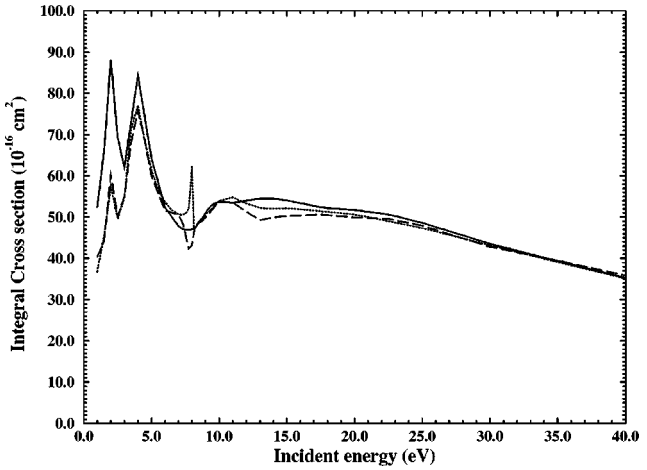

FIG. 8. Integral cross section for e^--CCl_4 scattering. Solid line: basis C (147-function calculation). Long-dashed line: basis A (115-function calculation). Dotted line: basis B (Ref. [7]).

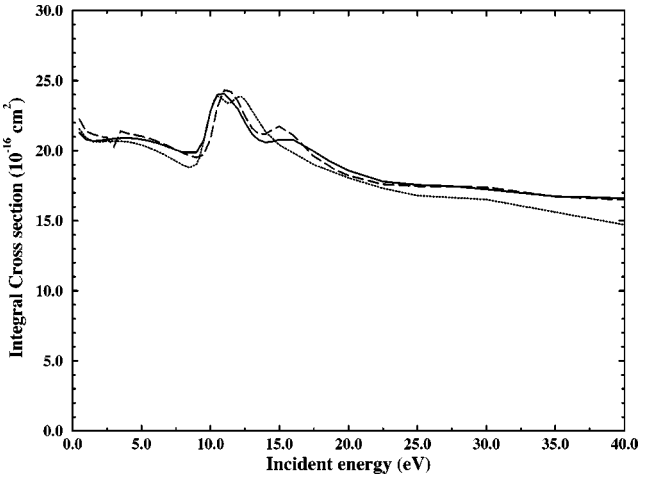

FIG. 9. Integral cross section for e^--CF_4 scattering. Solid line: basis C (126-function calculation). Long-dashed line: basis A (111-function calculation). Dotted line: basis B (Ref. [7]).

with a lager basis set for the Cl atom, shown in Table III. Since we again excluded the symmetric combinations of *d* Gaussians, the trial scattering wave function was expanded in a 147-function basis set. In Fig. 8 we show the three calculations performed for e^--CCl_4 scattering: (i) basis A (present 115-function calculation); basis B (Ref. [7]); basis C (present 147-function calculation). It is clear that the cross section obtained with basis C shows no thin structure around 8.0 eV. One finds, however, good agreement among the three calculations. The discrepancy found between 1 eV and 3 eV indicates that the smaller basis sets were not able to describe the scattering process at such low energies. This aspect, however, is not important, since it is not feasible to obtain faithful cross sections at $E<3$ eV with SE calculations.

As we have pointed out, present ICS calculations (basis A) for CF_4 have also shown a thin structure at 3.0 eV (Fig. 1). It was caused by linear dependences of the same nature, and the above discussion also holds for this molecule. We have performed extra calculations with a 131-function scattering basis set, which was reduced to 126 functions due to the exclusion of the troublesome symmetric combinations of *d* Gaussians. We have used basis A for the C atom and the basis shown in Table III for the F atom. We show, in Fig. 9, our three pseudopotential ICS: (i) present 111-function calculation (basis A); (ii) previous 111-function calculation [7] (basis B); (iii) present 126-function calculation (basis C). It is clear that there is always very good agreement among the three curves. The broader structures (between 10.0 eV and 17.0 eV) provided by basis A are reproduced by basis C.

In Fig. 10, we compare differential elastic cross sections of CF_4 obtained with basis A (111 basis functions), B (Ref. [7]), and C (126 basis functions) at 5, 10, 15, and 35 eV. Experimental elastic cross sections of Boesten *et al.* [23] are also included. The three basis sets have provided very similar DCS. It is clear that the agreement between theory and experiment is also very good, especially for higher energies, where polarization effects are not important.

Finally, in Fig. 11 we compare elastic DCS for the XY_4 family at 7.5, 10, 15, 20, 25, and 30 eV. One should notice that DCS for the lightest system, CF_4, is quite dissimilar from the others. Such a behavior, due to the smaller size of fluorine atoms, has been previously observed in a compari-

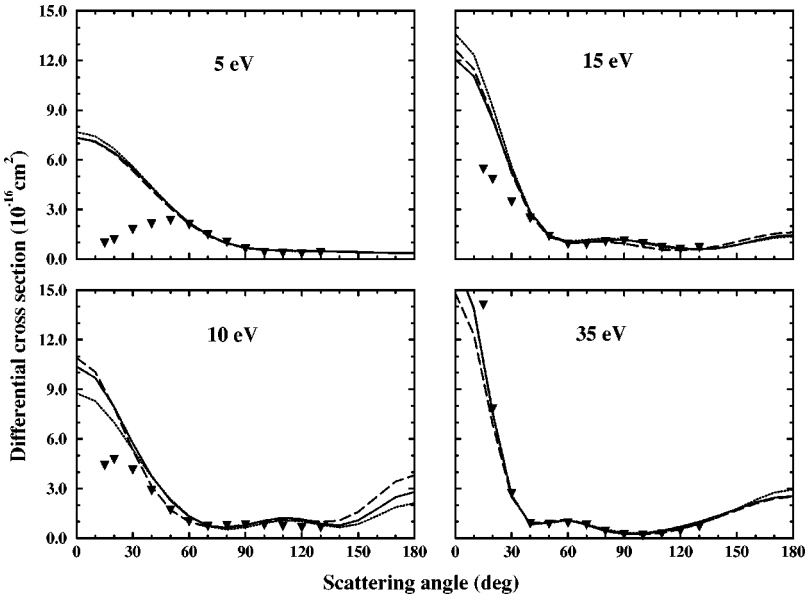

FIG. 10. Differential elastic cross section for e^--CF_4 scattering at 5, 10, 15, and 35 eV. Solid line: basis C (126-function calculation). Long-dashed line: basis A (111-function calculation). Dotted line: basis B (Ref. [7]); triangles: experimental data [23].

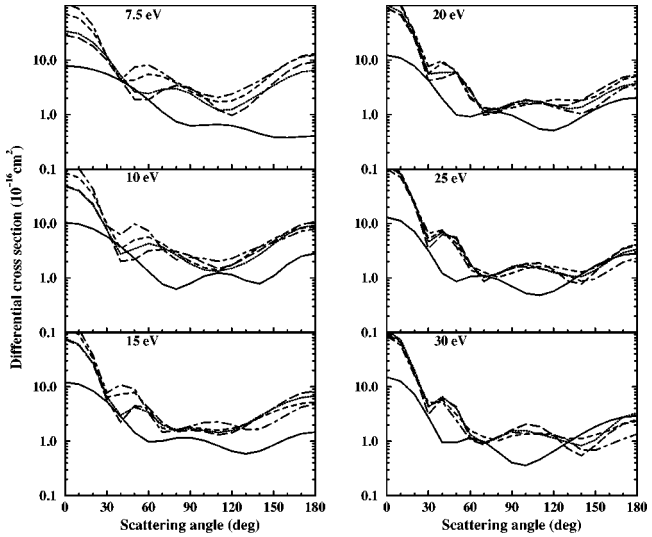

FIG. 11. Differential elastic cross section for XY_4 molecules. Solid line: CF_4; long-dashed line: CCl_4; dotted line: $SiCl_4$; short-dashed line: $SiCl_4$; dot-dashed line: SiI_4.

son between DCS for fluoromethanes and chloromethanes [28], and was to be expected. It is also to be noticed that CCl_4 and $SiCl_4$ cross sections are always very close, indicating that central atoms do not effectively act as scattering centers in such systems.

B. Rotational results

Since the elastic results obtained with basis A have always been better than those obtained with basis B, we decided to rotationally resolve the scattering amplitudes provided by basis A for $SiCl_4$ and $SiBr_4$. For CF_4, CCl_4, and SiI_4, we rotationally resolved the scattering amplitudes obtained with larger basis sets (126-function basis set for CF_4 and 147-function basis sets for CCl_4 and SiI_4). Partial-wave decompositions of the elastic amplitudes were truncated at $l=7$ for all targets. Integrations were carried out using Gauss-Legendre quadratures with 392 points (14 for $0 \leqslant \theta \leqslant \pi$ and 28 for $0 \leqslant \phi \leqslant 2\pi$).

In Table IV, we compare our elastic (unresolved) ICS and

TABLE IV. Elastic integral cross section (A) and rotationally summed integral cross section ($0 \rightarrow 0,3,4,6$) (B) for XY_4 (10^{-16} cm^2).

System		7.5 eV	10 eV	15 eV	20 eV	25 eV	30 eV
CF_4	(A)	20.06	22.84	20.79	18.58	17.55	17.25
	(B)	20.01	21.30	19.92	17.76	16.09	15.08
CCl_4	(A)	46.93	53.60	54.10	51.68	48.61	43.56
	(B)	44.57	48.01	47.49	45.86	43.64	38.02
$SiCl_4$	(A)	49.75	52.28	55.09	55.44	52.62	47.64
	(B)	47.65	46.64	47.18	47.51	44.38	38.45
$SiBr_4$	(A)	73.81	70.83	69.50	64.78	55.74	46.45
	(B)	67.07	62.29	60.94	55.88	46.16	35.94
SiI_4	(A)	92.47	88.36	79.59	67.29	53.43	42.21
	(B)	82.58	78.50	70.48	58.02	42.99	31.02

rotationally summed integral cross sections (RSICS), including $0 \rightarrow 0,3,4,6$ rotational transitions in the sums. We believe that results are reasonable, presenting the expected behavior. Both results agree within 12% at 7.5 and 10 eV, for all molecules. The largest discrepancy (26,5%) is found for SiI_4 at 30 eV. This is reasonable, since higher incident energies and larger molecules should couple higher angular momenta.

In Figs. 12 and 13, we show DCS for $0 \rightarrow 0$, $0 \rightarrow 3$, $0 \rightarrow 4$, and $0 \rightarrow 6$ transitions at the same energies. It is clear that structures (oscilations and minima) become more striking when the size of the peripheral atoms is increased. For a given molecule, cross sections are smoother at lower energies. In particular, CF_4, which is the lighter system, once more presents a distinguished behavior, with smoother cross sections at all energies and also with lower rotationally inelastic cross sections. This feature is confirmed by integral cross sections (ICS), which are shown in Table V. The study of XH_4 molecules (X:C, Si, Ge, Sn, and Pb) [11] has indicated that molecular shape—or, more specifically, molecular sphericity—plays a relevant role in the scattering process. Highly spherical molecules interact with incident particles through an almost spherically symmetric potential, therefore leading to smaller inelastic cross sections. (Remember that a spherically symmetric interaction potential causes the target's angular momentum to be a constant of the motion,

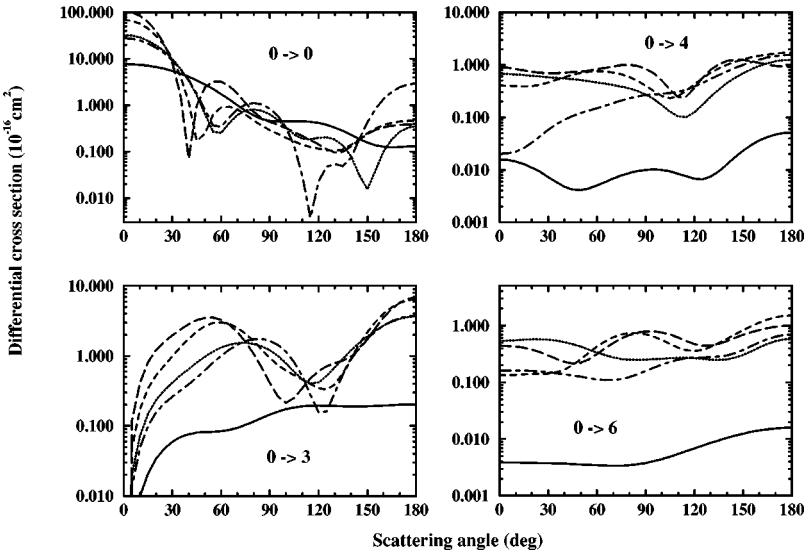

FIG. 12. Rotationally resolved DCS for e^--XY_4 scattering, considering $0 \rightarrow 0$, $0 \rightarrow 3$, $0 \rightarrow 4$, and $0 \rightarrow 6$ excitations at impact energy of 7.5 eV. Solid line: CF_4. Dot-dashed line: CCl_4. Dotted line: $SiCl_4$. Dashed line: $SiBr_4$. Long-dashed line: SiI_4.

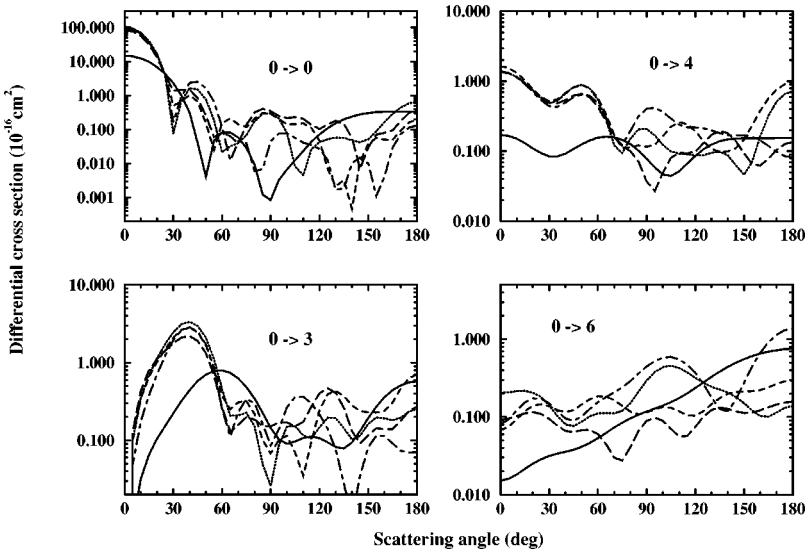

FIG. 13. Same as Fig. 12, but at 30 eV.

preventing rotational excitations from taking place.) Applying this statement to the molecules treated here, one could say that CF_4 is the most spherical system among XY_4 molecules. This was to be expected since the peripheral F atom is smaller than Cl, Br, and I.

TABLE V. Rotational integral cross sections ($J \rightarrow J'$) for XY_4 (10^{-16} cm^2).

System	$0\rightarrow0$	$0\rightarrow3$	$0\rightarrow4$	$0\rightarrow6$
7.5 eV CF_4	18.10	1.711	0.127	0.071
CCl_4	24.93	12.62	4.400	2.616
$SiCl_4$	25.28	13.26	4.976	4.134
$SiBr_4$	33.96	18.84	7.858	6.410
SiI_4	46.69	19.53	9.666	6.695
10 eV CF_4	15.76	1.811	2.438	1.292
CCl_4	25.35	9.912	6.429	6.315
$SiCl_4$	23.17	13.65	5.165	4.655
$SiBr_4$	35.30	14.53	7.209	5.249
SiI_4	49.31	14.93	7.804	6.454
15 eV CF_4	12.14	4.750	1.730	1.302
CCl_4	29.91	8.325	4.162	5.091
$SiCl_4$	27.87	9.311	5.177	4.819
$SiBr_4$	37.92	10.78	7.129	5.112
SiI_4	44.83	13.24	7.165	5.244
20 eV CF_4	9.120	5.434	1.686	1.523
CCl_4	28.58	8.093	4.363	4.827
$SiCl_4$	29.45	8.952	4.714	4.398
$SiBr_4$	36.08	9.999	6.308	3.493
SiI_4	38.32	10.94	5.811	2.948
25 eV CF_4	7.396	4.865	1.690	1.143
CCl_4	26.68	8.151	4.824	3.988
$SiCl_4$	28.25	8.087	4.080	3.959
$SiBr_4$	29.65	8.932	4.915	2.662
SiI_4	28.51	8.334	4.339	1.808
30 eV CF_4	7.604	3.796	1.392	2.287
CCl_4	23.12	6.763	4.227	3.908
$SiCl_4$	24.36	7.653	3.690	2.743
$SiBr_4$	22.63	7.252	4.229	1.830
SiI_4	20.70	6.241	3.071	1.005

Another interesting point revealed by ICS is the fact that XY_4 molecules present high inelastic rotational cross sections. The sums of $0\rightarrow3$, $0\rightarrow4$, and $0\rightarrow6$ ICS are always comparable in magnitude with the elastic ones. We have estimated the mean rotational energy transfer per collision for XY_4 molecules at 7.5 eV, following the procedure described in Ref. [15]. The mean rotational energy transfer is temperature-independent, and may therefore be applied to real gases. The results, shown in Table VI, indicate 10^{-5} eV as a typical value of pure rotational energy transfer per collision. Although this is a small number compared to the typical vibrational energy transfer, the rotational energy transfer in gaseous discharge environments may be relevant, since a single electron usually experiences 10^9 collisions per second in a cold plasma.

Finally, we observe that rotationally inelastic cross sections of methane and silane [11] are always smaller than, respectively, those of CX_4 (X:F, Cl) and SiY_4 (Y:Cl, Br, I). In order to ilustrate this point, we show, in Table VII, rotationally elastic (RE) ICS and inelastic rotationally summed (IRS) ICS for CX_4 (X:H, F, Cl) and SiY_4 (Y:H, F, Cl, Br, and I) at 7.5 and 30 eV. In the sums, we have considered only $0\rightarrow3,4$ rotational exitations. It is clear that heavier peripheral atoms, especially Cl, Br, and I, provide larger rotationally inelastic cross sections than H.

IV. CONCLUSIONS

In general, the fixed-nuclei static-exchange (SE) results obtained with both basis sets (A and B) are in good agreement. Whenever it was necessary to perform calculations

TABLE VI. Mean rotational energy transfer per collision for XY_4 family at 7.5 eV in a room-temperature gas ($T=300$ K).

System	$\langle\Delta E\rangle$ (10^{-5} eV)
CF_4	3.09
CCl_4	9.64
$SiCl_4$	4.91
$SiBr_4$	1.80
SiI_4	0.89

TABLE VII. Rotationally elastic (RE) and inelastic rotationally summed (IRS) ($0\rightarrow3,4$) ICS (10^{-16} cm^2) for CX_4 (X:H, F, Cl) and SiY_4 (Y:H, Cl, Br, I) molecules.

Energy (eV)	System	RE	IRS
	CH_4	17.77	1.436
7.5	CF_4	18.10	1.839
	CCl_4	24.93	17.02
	SiH_4	36.77	9.431
	$SiCl_4$	25.28	18.24
7.5	$SiBr_4$	33.96	26.70
	SiI_4	46.69	29.20
	CH_4	9.512	2.104
30	CF_4	7.604	5.188
	CCl_4	23.12	10.99
	SiH_4	11.32	1.601
	$SiCl_4$	24.36	11.34
30	$SiBr_4$	22.63	11.48
	SiI_4	20.70	9.312

with larger basis sets, we have also found excellent concordance. The thin structures found in the elastic integral cross sections (ICS) calculated with basis A (present) and basis B (Ref. [7]) were found to be spurious and related to linear dependences in the basis sets. Our elastic ICS generally agree in shape with experimental total cross sections for all XY_4 systems. For CF_4, there are experimental elastic ICS [23], which agree well with our results for incident energies beyond 10 eV. The concordance between experiment and theory for elastic DCS of CF_4 is very good. We therefore conclude, through the present application, that the Schwinger multichannel method with pseudopotentials is a powerful technique to study low-energy electron scattering by molecules with heavy atoms (and, at present, it is the only available one). The next challenging step is the application of this method to more complex studies including electronic excitation (open channels) and polarization effects (closed channels).

Our appreciation about the rotational results is also very positive. Unfortunately, comparisons could be made only through RSDCS, since there are no available rotationally resolved cross sections in the literature for the molecules we show in the present paper. The sum of $0\rightarrow0,3,4,6$ rotational excitations is enough to reasonably reproduce the rotationally unresolved elastic cross section, at least for $E<10$ eV. This is an important fact, since these state-to-state rotational cross sections are the fundamental information concerning pure rotational energy transfer in gaseous discharges. One should also remember that the measurement of rotationally resolved cross sections for such heavy molecules is a very hard task, and theoretical calculations are perhaps the only way to estimate them.

It was found that heavier peripheral atoms play a significant role as scattering centers. As a result, the molecules treated in this paper show high rotationally inelastic cross sections.

ACKNOWLEDGMENTS

M.T.N.V., M.H.F.B., and M.A.P.L. acknowledge partial support from the Brazilian agency Conselho Nacional de Desenvolvimento Científico e Tecnológico (CNPq). A.P.P.N. acknowledges support from Fundação de Amparo à Pesquisa do Estado de São Paulo (FAPESP). M.H.F.B. also acknowledges partial support from Fundação da Universidade Federal do Paraná para o Desenvolvimento da Ciência, da Tecnologia e da Cultura (FUNPAR). Our calculations were made at the Centro Nacional de Processamento de Alto Desempenho (CENAPAD–São Paulo).

[1] M. Hayashi, *Proceedings of the Meeting of the Fourth International Swarm Seminar and the Inelastic Electron-Molecule Collisions Symposium, July, 1985, Tahoe City, CA*, edited by L. C. Pitchford, B. V. McKoy, A. Chutpian, and S. Trajmar (Springer-Verlag, New York, 1987), p. 167.

[2] K. Takatsuka and V. McKoy, Phys. Rev. A **24**, 2473 (1981); **30**, 1734 (1984).

[3] T. N. Rescigno and B. I. Schneider, Phys. Rev. A **45**, 2894 (1992); T. N. Rescigno, B. H. Lengsfiel, C. W. McCurdy, and S. D. Parker, *ibid.* **45**, 7800 (1992).

[4] K. Pfingst, B. M. Nestmann, and S. D. Peyerimhoff, J. Phys. B **27**, 2283 (1994); B. M. Nestmann, K. Pfingst, and S. D. Peyerimhoff, *ibid.* **27**, 2297 (1994); L. A. Morgan, C. J. Gillian, J. Tennyson, and X. Cheng, *ibid.* **30**, 4087 (1997).

[5] M. H. F. Bettega, L. G. Ferreira, and M. A. P. Lima, Phys. Rev. A **47**, 1111 (1993).

[6] G. B. Bachelet, D. R. Hamann, and M. Schlüter, Phys. Rev. B **26**, 4199 (1982).

[7] A. P. P. Natalense, M. H. F. Bettega, L. G. Ferreira, and M. A. P. Lima, Phys. Rev. A **52**, R1 (1995).

[8] M. H. F. Bettega, A. P. P. Natalense, M. A. P. Lima, and L. G. Ferreira, J. Chem. Phys. **103**, 10 566 (1995).

[9] A. P. P. Natalense, C. S. Sartori, L. G. Ferreira, and M. A. P. Lima, Phys. Rev. A **54**, 5435 (1996).

[10] A. P. P. Natalense, L. G. Ferreira, and M. A. P. Lima, Phys. Rev. Lett. **81**, 3832 (1998).

[11] M. T. do N. Varella, M. H. F. Bettega, and M. A. P. Lima, Z. Phys. D **39**, 59 (1997).

[12] M. T. do N. Varella, M. H. F. Bettega, A. J. R. da Silva, L. G. Ferreira, and M. A. P. Lima, J. Chem. Phys. **110**, 2452 (1999).

[13] K. Jung, Th. Antoni, R. Müller, K.-H. Kochem, and H. Ehrhardt, J. Phys. B **15**, 3535 (1982).

[14] R. Müller, K. Jung, K.-H. Kochem, W. Sohn, and H. Ehrhardt, J. Phys. B **18**, 3971 (1985).

[15] A. Jain, Z. Phys. D **21**, 153 (1991).

[16] M. A. P. Lima and V. McKoy, Phys. Rev. A **38**, 501 (1988).

[17] M. A. P. Lima, L. M. Brescansin, A. J. R. da Silva, C. Winstead, and V. McKoy, Phys. Rev. A **41**, 327 (1990).

[18] L. M. Brescansin, M. A. P. Lima, and V. McKoy, Phys. Rev. A **40**, 5577 (1989).

[19] M. E. Rose, *Elementary Theory of Angular Momentum* (Wiley, New York, 1957).

[20] M. H. F. Bettega, A. P. P. Natalense, M. A. P. Lima, and L. G. Ferreira, Int. J. Quantum Chem. **60**, 821 (1996).

[21] C. Winstead, Q. Sun, and V. McKoy, J. Chem. Phys. **98**, 1105 (1993).
[22] W. A. Isaacs, W. McCurdy, and T. N. Rescigno, Phys. Rev. A **58**, 309 (1998).
[23] L. Boesten, H. Tanaka, A. Kobayashi, M. A. Dillon, and M. Kimura, J. Phys. B **25**, 1607 (1992).
[24] O. Sueoka, S. Mori, and A. Hamada, J. Phys. B **27**, 1453 (1994).
[25] C. Szmytkowski, A. Krzysztofowicz, P. Janicki, and L. Rosenthal, Chem. Phys. Lett. **199**, 191 (1992).
[26] F. A. Gianturco, R. R. Lucchese, and N. Sanna, J. Chem. Phys. **104**, 6482 (1996).
[27] Hai-Xing Wan, J. H. Moore, and J. A. Tossell, J. Chem. Phys. **91**, 7340 (1989).
[28] A. P. P. Natalense, M. H. F. Bettega, L. G. Ferreira, and M. A. P. Lima, Phys. Rev. A **59**, 879 (1999).